

# Normal mode analysis as a prerequisite for drug design: Application to matrix metalloproteinases inhibitors

Nicolas Floquet<sup>a</sup>, Jean-Didier Marechal<sup>b</sup>, Marie-Ange Badet-Denisot<sup>a</sup>, Charles H. Robert<sup>b</sup>,  
Manuel Dauchez<sup>c</sup>, David Perahia<sup>b,\*</sup>

<sup>a</sup> Institut de Chimie des Substances Naturelles (ICSN), CNRS UPR-2301, Bat. 27 Avenue de la Terrasse, 91198 Gif sur Yvette, France

<sup>b</sup> Laboratoire de Modélisation et d'Ingénierie des Protéines, Université Paris-Sud, 91405 Orsay, France

<sup>c</sup> Laboratoire de Biochimie Médicale et Biologie Moléculaire, CNRS UMR 6198, IFR 53 Biomolécules, Université de Reims-Champagne-Ardenne, France

Received 11 July 2006; revised 4 August 2006; accepted 14 August 2006

Available online 1 September 2006

Edited by Miguel De la Rosa

**Abstract** We demonstrate the utility of normal mode analysis in correctly predicting the binding modes of inhibitors in the active sites of matrix metalloproteinases (MMPs). We show the accuracy in predicting the positions of MMP-3 inhibitors is strongly dependent on which structure is used as the target, especially when it has been energy minimized. This dependency can be overcome by using intermediate structures generated along one of the normal modes previously calculated for a given target. These results may be of prime importance for further *in silico* drug discovery.

© 2006 Federation of European Biochemical Societies. Published by Elsevier B.V. All rights reserved.

**Keywords:** Matrix metalloproteinases; MMPs; Normal mode analysis (NMA); Docking; Target flexibility

## 1. Introduction

Matrix metalloproteinases (MMPs) constitute a large family of secreted zinc-dependent proteases that degrade components of the extra-cellular matrix (ECM) [1]. They play a fundamental role in many physiological and pathological processes that involve connective tissue remodelling, including tumor angiogenesis, differentiation and metastasis [1–4]. The production and activity of many MMPs have been correlated with almost all types of cancers. Therefore, MMPs are important therapeutic targets and the search for efficient inhibitors represents an important field of investigation [5,6].

Among MMPs, MMP-3 has been extensively studied and many structures are available describing the unbound enzyme (PDB: 1CQR) [7] and different inhibitor-bound forms. Among the latter, we note the availability of the complex between MMP-3 and its physiological inhibitor, TIMP-1 (1UEA) [8].

Many other structures also describe the MMP-3 bound to piperazine (1D8F) [9], carboxylic acid (1HY7) [10], thiazepine (1D5J) [11] and pyrimidine based inhibitors (1G4K) [12]. All these inhibitors chelate the catalytic zinc ion and also fill a hydrophobic cavity in close proximity to the metal (S1' cavity). In the uninhibited enzyme structure, the S1' cavity is completely covered by Tyr223, while in the protein–inhibitor complexes, the inhibitors displace this residue in order to fit into the cavity.

Molecular (*in silico*) dockings are now tools widely used in drug design whether for spotting possible lead compounds or optimizing protein–drug interactions. In many current studies, molecular docking involves the prediction of ligand conformation and orientation within a rigid target binding site. When an X-ray crystal structure of the target is available, virtual high-throughput screening experiments can also be used to identify new hits by docking the 3D structures of molecules contained in a database.

In the case of MMP-3, using the crystal structure of the unbound enzyme is not suitable for docking experiment since the S1' cavity is narrower than in the bound form. On the other hand, using a structure from one of the available protein–inhibitor complexes could influence the docking results because the S1' cavity may be altered due to the presence of the corresponding ligand. To eliminate this bias, the ligand can be removed and the empty receptor submitted to energy minimization, molecular dynamics, and/or other molecular mechanics techniques. However, such methods when applied to the empty protein can lead to significant structural modifications resulting into inappropriate structures for docking experiment (e.g. those in which the binding site is closed). Thus, choosing an appropriate structure of the target for docking is not an easy task and requires particular attention.

A closely related problem in computational drug design is the difficulty of treating the flexibility of the target explicitly [13,14]. The use of only a single, rigid structure of the target can considerably reduce the chances of identifying new molecules that bind to the active site. Such a problem was recently addressed for MMPs [15]. Different approaches can be used to overcome this problem, including new algorithms that consider partial flexibility of the target [16]. Another approach is to use molecular dynamics simulations [17]. Recently, receptor flexibility in ligand docking was also considered using normal mode analysis (NMA) through a measure of relevance on a given region of interest [18].

\*Corresponding author. Fax: +33 1 69 85 37 15.  
E-mail address: [david.perahia@ibbmc.u-psud.fr](mailto:david.perahia@ibbmc.u-psud.fr) (D. Perahia).

**Abbreviations:** NMA, normal mode analysis; MMPs, matrix metalloproteinases; TIMPs, tissue inhibitors of MMPs; ECM, extra-cellular matrix; SD, steepest descent; ABNR, adopted basis Newton–Raphson; PDB, protein data bank; RMSD, root mean square deviation

In this study we performed a normal modes analysis on the MMP-3 catalytic domain from 1UEA. We visually inspected the 25 lowest frequency modes of vibration. As expected the first few modes presented the most collective motions, of which only one affected the binding-site cavity in a clear opening–closing fashion (mode number 2). Although other modes also modulated the geometry of the binding-site cavity, their effects were not as pronounced and therefore only mode 2 was selected for subsequent analysis. No further measure of relevance was deemed necessary such as that employed in Ref. [18]. Conformational search along additional modes or in combination may provide advantages in general but did not prove necessary in this case.

Using Flexx and Gold, two of the most efficient and commonly applied docking programs, we show that simply using the energy-minimized structure of MMP-3 from 1UEA [8] as the target indeed leads to unreliable positions of all of the ligands from the 1D8F, 1HY7, 1D5J and 1G4K complexes. On the contrary, structures obtained from NMA allowed us to dock correctly the various ligands using these programs.

We show that this strategy significantly improved the docking results and highlights the interest of applying NMA to drug design.

## 2. Materials and methods

### 2.1. Normal modes calculation

The MMP-3 catalytic domain structure considered for the NMA was taken from the MMP-3:TIMP-1 complex (1UEA) [8]. Zinc ions were included as given in the PDB structure and the calculations were performed after removal of the ligand from the active site. The hydrogen atoms were first built and the whole structure was energy minimized using the CHARMM program [19] and the force field PARAM22 [20] by using successively steepest descent (SD) and Adopted Basis Newton–Raphson (ABNR) algorithms. Harmonic constraints were applied to all the atoms, whose force constants were progressively decreased from 250 to 0 kcal mol<sup>−1</sup> Å<sup>−2</sup> during SD minimization. A final minimization with all constraints removed was performed using ABNR until a root mean square energy gradient of 10<sup>−6</sup> kcal mol<sup>−1</sup> Å<sup>−1</sup> was reached. The normal modes were computed with the DIMB method [21] as implemented in CHARMM. For each system, the lowest frequency modes were computed with a convergence criterion of 10<sup>−4</sup> on eigenvectors. Electrostatic interactions were treated with a *r*-dependent dielectric constant and a switch function applied between 10.0 and 12.0 Å. Less than 5 h CPU-time were required on a linux PC 3.4 GHz/2 Go RAM to obtain the description of the 100 lowest frequencies normal modes of MMP-3 as well as the intermediate structures along one mode direction.

### 2.2. Docking

The different MMP structures considered (1D8F, 1HY7, 1D5J, 1G4K) were superimposed on that of 1UEA in order to obtain the coordinates of ligands and of the protein targets in the same orientation as 1UEA. Root mean square differences (RMSD) for the different pairs of structures are reported in Table 1 which shows highly similar structures. Nevertheless, the 1UEA structure was found to be significantly different from the others.

For each ligand, hydrogen atoms were added, charges were assigned with Sybyl (©Tripos) and a short energy minimization was achieved using the Tripos Force field [22].

Thereafter, all the ligands were docked into all the MMP-3 structures employing either the Flexx program [23] and its scoring function [24,25] as available in the Sybyl graphical interface, or the Gold program [26] using the Goldscore scoring function [27].

The ligands were docked within a sphere of 15 Å around the catalytic zinc ion located in the active site and that participates in ligand binding. The default parameters of the two programs were used for

Table 1

Cross RMSD table of the MMP-3 structures used for the study

	1UEA	1D8F	1G4K	1HY7	1D5J
1UEA	0	1.85	1.77	1.73	1.79
1D8F	–	0	0.54	0.37	0.51
1G4K	–	–	0	0.41	0.55
1HY7	–	–	–	0	0.56
1D5J	–	–	–	–	0

The RMSD were computed on the main chain atoms. The structure 1UEA is the most divergent from the others. This structure was used for NMA.

docking. The 30 best solutions for each docked ligand were conserved for analysis.

The figures were realized using VMD [28] and Pymol (©Delano Scientific LLC) available at <http://pymol.sourceforge.net/>.

## 3. Results

To validate both Gold and Flexx docking approaches and to examine their ability to correctly identify the ligand positions in the MMP-3:ligands complexes, we first docked the ligands from 1D8F, 1HY7, 1D5J and 1G4K in their corresponding X-ray structures, as well as in the structure of MMP-3 from 1UEA.

The ligand positions proposed by Flexx and Gold were sorted according to their RMSD from the corresponding crystallographic position of the ligands, when available. It was observed that both methods were able to correctly predict the position of each ligand when using its corresponding protein X-ray structure, and also most of the other available structures as targets (Fig. 1). However, when using 1UEA as a target, we note that Flexx was only able to correctly replace one ligand (1D8F) out of four, showing the limits of docking a ligand in an inappropriate structure, even if highly related. In the same conditions, Gold successfully replaced all four ligands. We conclude that Gold is more permissive than Flexx in taking into account some structure variability.

Using the crystal structure of a protein complexed with a particular ligand as a target for docking another ligand introduces a potential bias into the procedure. An unbiased docking protocol should take the unliganded structure, if available, as target, as in protein–protein docking predictions undertaken in the CAPRI trials [29]. An alternative is to remove the existing ligand and apply energy minimization or other molecular mechanics techniques to the structure in order to partially reverse any ligand-induced changes.

After energy minimization of the empty 1UEA structure, neither Flexx nor Gold was able to correctly predict the binding modes of any of the ligands. In Fig. 2A, the tube colour and diameter represents the RMSD values obtained by comparing the initial and energy-minimized structures from 1UEA; this shows that the failure of the docking is probably due to conformational differences observed in the region of the active site (black arrows) leading to its partial closure, especially in the region of the S1' hydrophobic pocket (Fig. 2B).

A NMA was then performed on the structure of MMP-3 from 1UEA. Interestingly, it was observed that the second-lowest-frequency vibrational mode corresponded to internal motions describing the opening and the closure of the active

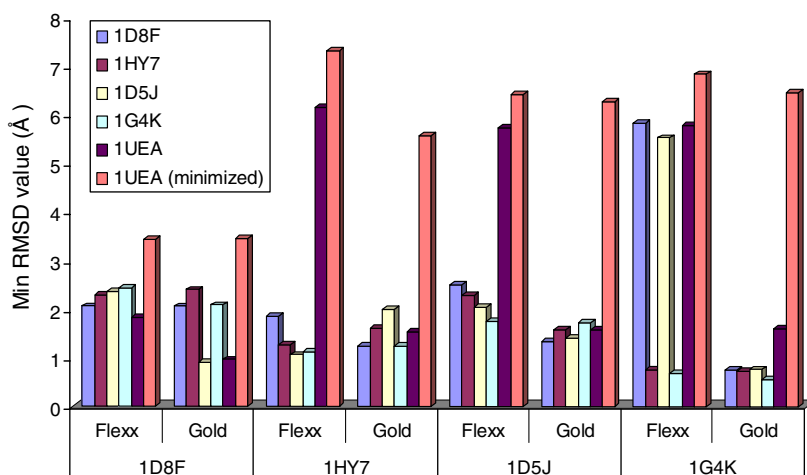


Fig. 1. Results obtained with Flexx and Gold by docking the ligands from the different MMP-3 PDB structures into all the X-ray structures taken as targets, and also into the 1UEA X-ray and energy-minimized structures.

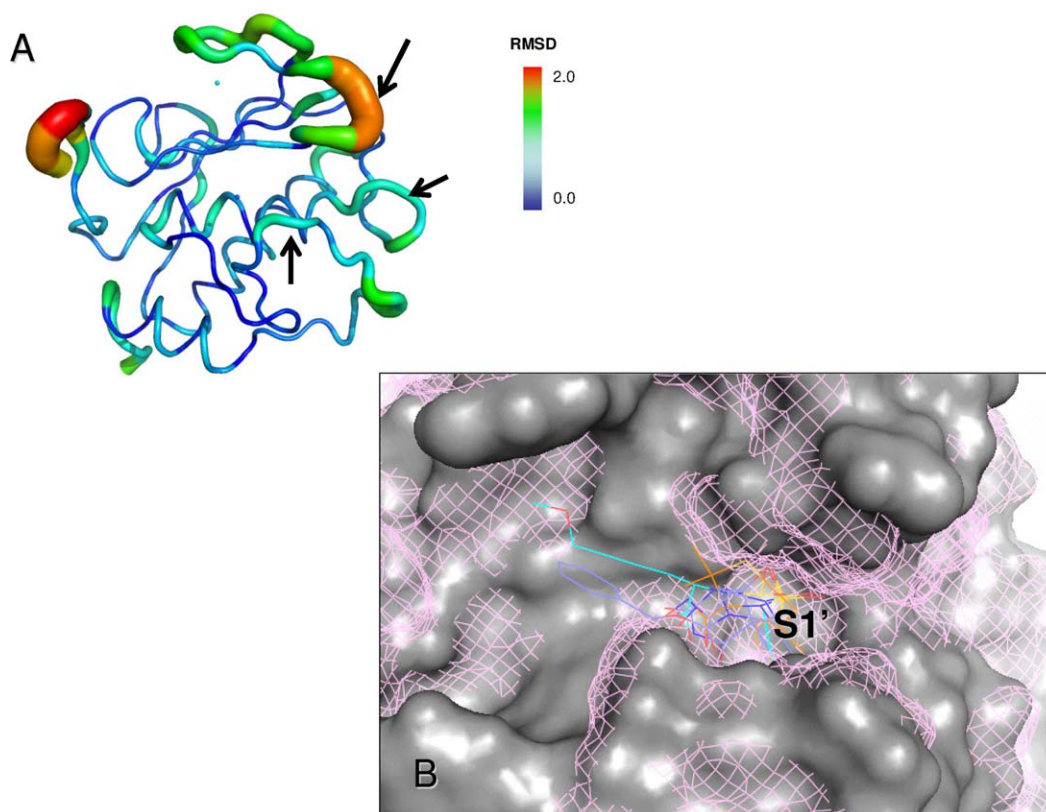


Fig. 2. Structural differences observed after energy minimization of the MMP-3 catalytic domain from 1UEA. (A) RMSD deviations with respect to the X-ray structure represented by coloured ribbon that shows the deviations in the region of the active site (Global RMSD on heavy atoms = 1.4 Å). (B) Accessible surface in the region of the active site: pink meshes and the solid surface stand for the minimized and for the X-ray structures, respectively. The MMP-3 ligands are shown as thin lines. The binding site, in particular the S1' pocket, can be seen to narrow after minimization.

site of the metalloproteinase. A representation of the movements of the C $\alpha$  atoms of the protein along this mode is shown in Fig. 3A. Accordingly, we further examined the potential role of such a movement on the results of docking experiments applied to metalloproteinases.

A total of 11 intermediate structures of the MMP-3 from 1UEA were then obtained for different values of the normal coordinate along this particular mode in the opening direction. These structures were further used as successive targets for docking. They corresponded to displacements ranging from

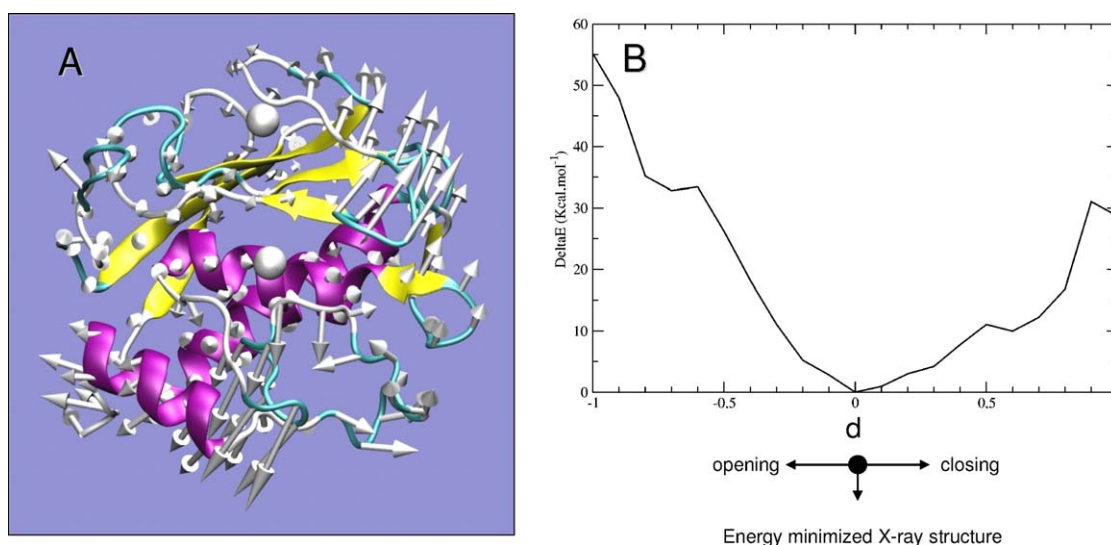


Fig. 3. (A) 2D representation of the C $\alpha$  atom movements (shown with arrows) of MMP-3 from 1UEA along the second lowest-frequency mode (3.8 cm<sup>-1</sup>) corresponding to internal motions as determined by NMA and describing the opening and the closure of the active site. (B) Variations of energies of the corresponding intermediate minimized structures under NM restraint potential with respect to the X-ray energy-minimized structure ( $d_r = 0$  Å).

0.0 to 1.0 Å with steps of 0.1 Å with respect to the initial X-ray minimized structure and were obtained by energy minimization using a restraint potential added to the internal standard potential of the form:

$$k/2(d - d_r)^2$$

where  $d$  is the displacement along the normal mode coordinate corresponding to the given mode (here mode 2),  $d_r$  the desired restraint distance value and  $k$  the force constant (500,000 kcal mol<sup>-1</sup> Å<sup>-2</sup>).  $d$  is defined by projecting the vector of mass weighted coordinate differences (with respect to the energy-minimized conformation) onto the normal mode vector. Two other restraint potentials were added corresponding to the restriction of overall rotational and translational motions of the molecule as described in Guilbert et al. [30].

The restraint potential allows one to obtain a series of low-energy structures along the normal mode direction without being limited by the harmonic approximation inherent to NMA. Thus, the series of structures corresponded well to dif-

ferent magnitudes of the opening of the cleft as described by the mode 2. The minimizations were carried out by successively combining the SD and ABNR methods until an energy gradient of 10<sup>-6</sup> kcal mol<sup>-1</sup> Å<sup>-1</sup> was reached. The energies corresponding to these structures are shown in Fig. 3B. It may be noted that reasonable energy deviations of less than 50 kcal mol<sup>-1</sup> up to about 1 Å displacement were observed.

By considering intermediate structures of MMP-3 along mode 2 as targets, three out of four ligands were correctly predicted with Flexx, as shown in Fig. 4. This corresponds to a remarkable improvement as it was impossible for Flexx to predict the correct binding modes of three out of four ligands in the initial X-ray structure, as seen above. Moreover, for each ligand, the best solution, as measured by the RMSD from the crystallographic model, was found in the ten best scores proposed by the software.

To illustrate the results obtained with Gold, we report in Fig. 5 the best (min RMSD) position of each ligand when docked into the X-ray energy-minimized structure from

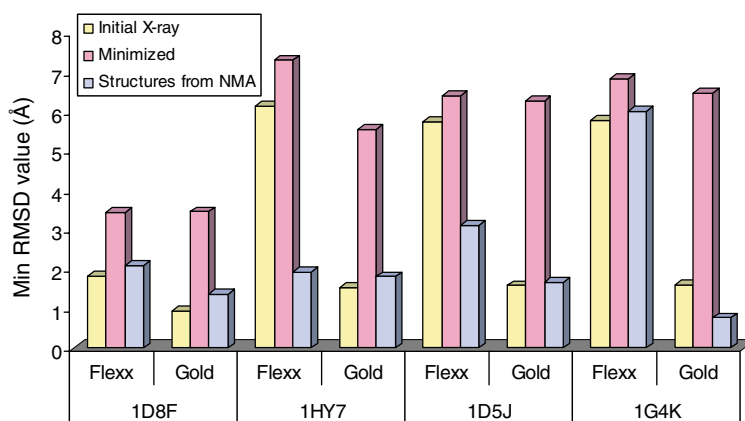


Fig. 4. Results of the docking of the ligands with Flexx and Gold in the initial X-ray structure from 1UEA, in the corresponding minimized structure, and in the set of energy-minimized structures generated along mode 2 in the opening direction.



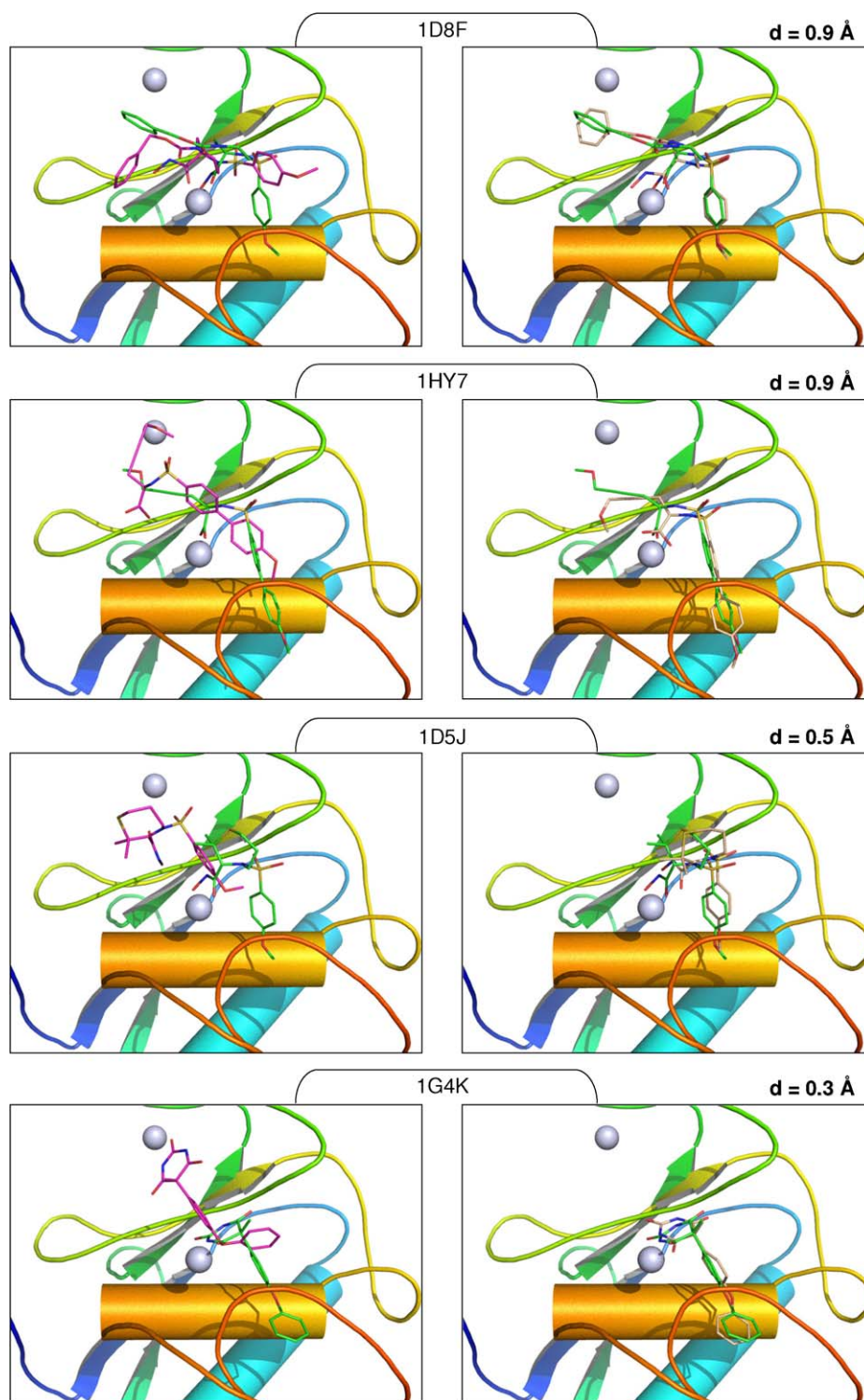


Fig. 5. Graphical models of the minimum RMSD solutions proposed by Gold after the docking of the four ligands; left: in the X-ray energy-minimized structure from the PDB 1UEA; right: in one of the intermediate structures generated along mode 2 in the opening direction. In each case, the crystallographic solution is shown in green.

1UEA (left), and into the set of intermediate structures generated along mode 2 in the opening direction (right). The crystallographic position of the ligand is shown in green. In each case, the value of  $d$  (displacement along the mode) for which the minimum RMSD of the ligand was found is given. With Gold,

all four ligands were successfully predicted leading to results very close to those obtained by crystallography. Thus, for Gold, the NMA approach was not as necessary as for Flexx when docking to the initial X-ray structure. However, the NMA methodology considerably improved the docking results

as compared to those obtained with the X-ray energy-minimized structure. Accordingly, with Gold, this approach was particularly useful when starting from an unbiased, ligand-free structure. Moreover, we observed that in some cases, the position of the ligand may be slightly improved as compared to the prediction starting with the liganded structure, as was observed for the 1G4K ligand.

#### 4. Discussion

When the structure of a particularly interesting pharmaceutical target has been resolved, ligand docking is often applied in order to predict the binding mode of a ligand or to identify new inhibitors from a database. Currently, such docking usually implies a flexible ligand and a rigid target. Difficulties commonly arise when the flexibility of the target itself is significant. A possible solution to overcome this flexibility problem would be to dock every ligand in each known receptor structure. In the case of MMPs, the unliganded enzyme exhibits an active site that is totally buried, making this structure unsuitable for docking experiments. Additionally, for many MMPs only one structure has been resolved; such a structure may be essentially biased because it describes the target bound to a specific ligand.

In general, both to get an unbiased structure and to be able to apply any number of molecular modelling/molecular mechanics techniques, the initial X-ray structure needs to be properly energy minimized. The resulting structure is not necessarily appropriate for ligand binding using existing techniques. Furthermore, for most MMPs, no crystal structure is available and the only targets are obtained by homology modelling, which usually involves energy minimization and/or conformational sampling by molecular dynamics simulations [31].

Protein motions associated with ligand binding comprise in general both local and global components. We show here that NMA is very useful to explore collective movements of functional relevance and thereby provide structures that can be more appropriate for docking. On the other hand, side-chain flexibility can be sufficient to open binding-site cavities to ligand access as was the case with the S1' cavity in MMP-1 [15]. While such local approaches will miss larger scale modifications (e.g. backbone movements), the approach presented here may underestimate local rearrangements. The local and global approaches can be viewed as complementary in improving modelling of protein–ligand interactions.

#### References

- [1] Sternlicht, M.D. and Werb, Z. (2001) How matrix metalloproteinases regulate cell behavior. *Annu. Rev. Cell Dev. Biol.* 17, 463–516.
- [2] Lochter, A., Sternlicht, M.D., Werb, Z. and Bissell, M.J. (1998) The significance of matrix metalloproteinases during early stages of tumor progression. *Ann. NY Acad. Sci.* 857, 180–193.
- [3] Handsley, M.M. and Edwards, D.R. (2005) Metalloproteinases and their inhibitors in tumor angiogenesis. *Int. J. Cancer* 115, 849–860.
- [4] Bjorklund, M. and Koivunen, E. (2005) Gelatinase-mediated migration and invasion of cancer cells. *Biochim. Biophys. Acta* 1755, 37–69.
- [5] Itoh, Y. and Nagase, H. (2002) Matrix metalloproteinases in cancer. *Essays Biochem.* 38, 21–36.
- [6] Mannello, F., Tonti, G. and Papa, S. (2005) Matrix metalloproteinase inhibitors as anticancer therapeutics. *Curr. Cancer Drug Targets* 5, 285–298.
- [7] Cheng, M., Rydel, T.J., Gu, F., Dunaway, C.M., Pikul, S., Dunham, K.M. and Barnett, B.L. (1999) Crystal structure of the stromelysin catalytic domain at 2.0 angstroms resolution: inhibitor-induced conformational changes. *J. Mol. Biol.* 293, 545–557.
- [8] Gomis-Ruth, F.X., Maskos, K., Betz, M., Bergner, A., Huber, R., Suzuki, K., Yoshida, N., Nagase, H., Brew, K., Bourenkov, G.P., Bartunik, H. and Bode, W. (1997) Mechanism of inhibition of the human matrix metalloproteinase stromelysin-1 by TIMP-1. *Nature* 389, 77–81.
- [9] Cheng, M., De, B., Pikul, S., Almstead, N.G., Natchus, M.G., Anastasio, M.V., McPhail, S.J., Snider, C.E., Taiwo, Y.O., Chen, L., Dunaway, C.M., Gu, F., Dowty, M.E., Mielsing, G.E., Janusz, M.J. and Wang-Weigand, S. (2000) Design and synthesis of piperazine-based matrix metalloproteinase inhibitors. *J. Med. Chem.* 43, 369–380.
- [10] Natchus, M.G., Bookland, R.G., De, B., Almstead, N.G., Pikul, S., Janusz, M.J., Heitmeyer, S.A., Hookfin, E.B., Hsieh, L.C., Dowty, M.E., Dietsch, C.R., Patel, V.S., Garver, S.M., Gu, F., Pokross, M.E., Mielsing, G.E., Baker, T.R., Foltz, D.J., Peng, S.X., Bornes, D.M., Stojnowski, M.J. and Taiwo, Y.O. (2000) Development of new hydroxamate matrix metalloproteinase inhibitors derived from functionalized 4-aminoprolines. *J. Med. Chem.* 43, 4948–4963.
- [11] Almstead, N.G., Bradley, R.S., Pikul, S., De, B., Natchus, M.G., Taiwo, Y.O., Gu, F., Williams, L.E., Hynd, B.A., Janusz, M.J., Dunaway, C.M. and Mielsing, G.E. (1999) Design, synthesis, and biological evaluation of potent thiazine- and thiazepine-based matrix metalloproteinase inhibitors. *J. Med. Chem.* 42, 4547–4562.
- [12] Dunten, P., Kammlott, U., Crowther, R., Levin, W., Foley, L.H., Wang, P. and Palermo, R. (2001) X-ray structure of a novel matrix metalloproteinase inhibitor complexed to stromelysin. *Protein Sci.* 10, 923–926.
- [13] Ferrari, A.M., Wei, B.Q., Costantino, L. and Shoichet, B.K. (2004) Soft docking and multiple receptor conformations in virtual screening. *J. Med. Chem.* 47, 5076–5084.
- [14] Rosenfeld, R., Vajda, S. and DeLisi, C. (1995) Flexible docking and design. *Annu. Rev. Biophys. Biomol. Struct.* 24, 677–700.
- [15] Alberts, I.L., Todorov, N.P. and Dean, P.M. (2005) Receptor flexibility in de novo ligand design and docking. *J. Med. Chem.* 48, 6585–6596.
- [16] Osterberg, F., Morris, G.M., Sanner, M.F., Olson, A.J. and Goodsell, D.S. (2002) Automated docking to multiple target structures: incorporation of protein mobility and structural water heterogeneity in AutoDock. *Proteins* 46, 34–40.
- [17] Sivanesan, D., Rajnarayanan, R.V., Doherty, J. and Pattabiraman, N. (2005) In-silico screening using flexible ligand binding pockets: a molecular dynamics-based approach. *J. Comput. Aided Mol. Des.* 19, 213–228.
- [18] Cavasotto, C.N., Kovacs, J.A. and Abagyan, R.A. (2005) Representing receptor flexibility in ligand docking through relevant normal modes. *J. Am. Chem. Soc.* 127, 9632–9640.
- [19] Brooks, B.R., Brucoleri, R.E., Olafson, B.D., States, D.J., Swaminathan, S. and Karplus, M. (1983) CHARMM: A Program for Macromolecular Energy, Minimization, and Dynamics Calculations. *J. Comp. Chem.* 4, 187–217.
- [20] MacKerell, A.D., Bashford, D., Bellott, M., Dunbrack, R.L., Evanseck, J.D., Field, M.J., Fischer, S., Gao, J., Guo, H., Ha, S., Joseph-McCarthy, D., Kuchnir, L., Kuczera, K., Lau, F.T.K., Mattos, C., Michnick, S., Ngo, T., Nguyen, D.T., Prodhom, B., Reiher, W.E., Roux, B., Schlenkrich, M., Smith, J.C., Stote, R., Straub, J., Watanabe, M., Workiewicz-Kuczera, J., Yin, D. and Karplus, M. (1998) All-atom empirical potential for molecular modeling and dynamics Studies of proteins. *J. Phys. Chem. B* 102, 3586–3616.
- [21] Perahia, D. and Mouawad, L. (1995) Computation of low-frequency normal modes in macromolecules: improvements to the method of diagonalization in a mixed basis and application to hemoglobin. *Comput. Chem.* 19, 241–246.
- [22] Clark, M., Cramer III, R.D. and van Opdenbosch, N. (1989) Validation of the general purpose Tripos 5.2 force field. *J. Comp. Chem.* 10, 982–1012.

- [23] Rarey, M., Kramer, B., Lengauer, T. and Klebe, G. (1996) A fast flexible docking method using an incremental construction algorithm. *J. Mol. Biol.* 261, 470–489.
- [24] Bohm, H.J. (1994) The development of a simple empirical scoring function to estimate the binding constant for a protein–ligand complex of known three-dimensional structure. *J. Comput. Aided Mol. Des.* 8, 243–256.
- [25] Klebe, G. (1994) The use of composite crystal-field environments in molecular recognition and the de novo design of protein ligands. *J. Mol. Biol.* 237, 212–235.
- [26] Verdonk, M.L., Cole, J.C., Hartshorn, M.J., Murray, C.W. and Taylor, R.D. (2003) Improved protein–ligand docking using GOLD. *Proteins* 52, 609–623.
- [27] Nissink, J.W., Murray, C., Hartshorn, M., Verdonk, M.L., Cole, J.C. and Taylor, R. (2002) A new test set for validating predictions of protein–ligand interaction. *Proteins* 49, 457–471.
- [28] Humphrey, W., Dalke, A. and Schulten, K. (1996) VMD: visual molecular dynamics. *J. Mol. Graph.* 14, 33–8, 27–8.
- [29] Janin, J. (2005) The targets of CAPRI rounds 3–5. *Proteins* 60, 170–175.
- [30] Guilbert, C., Perahia, D. and Mouawad, L. (1995) A method to explore transition in macromolecules. Applications to hemoglobin and phosphoglycerate kinase. *Comp. Phys. Commun.* 91, 263–273.
- [31] Sali, A. and Blundell, T.L. (1993) Comparative protein modelling by satisfaction of spatial restraints. *J. Mol. Biol.* 234, 779–815.